Experimental investigations on a grate incinerator of L-shaped flame fuelled by rural solid waste.

LIU, X., ASIM, T., ZHU, G., ZHANG, Y., MISHRA, R.

2019

COMADEM
International Journal of Condition Monitoring and Diagnostic Engineering Management

Experimental Investigations on a Grate Incinerator of L-shaped Flame Fuelled by Rural Solid Waste

Xiaozhou Liu [a], Taimoor Asim [b]*, Guangyu Zhu [a], Yu Zhang [a] and Rakesh Mishra [c]

[a] School of Material and Energy, Guangdong University of Technology, Guangzhou 510006, China
[b] School of Engineering, Robert Gordon University, Aberdeen, UK (AB10 7GJ)
[c] School of Computing & Engineering, University of Huddersfield, Huddersfield, UK (HD1 3DH)

* Corresponding author. Tel.: +44-1244-262457; email: t.asim@rgu.ac.uk

ABSTRACT

In this article, investigations on the structural parameters and aerodynamic characteristics of the furnace arches of a small scale L-shaped flame incinerator for the disposal of rural solid waste are carried out. A novel configuration of furnace arches for the incinerator of L-shaped flame is developed. Eight different test conditions are determined by using orthogonal experimental design method. Cold test with full coverage arch and sub-warehouse air supply are analyzed under eight different test conditions. Experimental results show that a stable combustion can be obtained by using L-shaped flame technology and the optimum air supply ratio between the front arch and the rear arch is discovered to be 3:7. It is found that the maximum turbulence intensity along the length of grate can reach 10%, and the burning exuberant zone is approximately 40%~75% of the whole relative length of the grate. The optimum dimensionless structural parameters of the furnace arch are: H/L = 0.333 and h/L = 0 .12 with the front arch angle of 45º. The effectiveness of configuration of arches as well as combustion air supply ratio for the L-shaped flame grate incinerator fueled by rural solid waste is verified by hot test.

Keywords: *Rural Solid Waste (RSW); Grate Incinerator; Air Supply Ratio; Turbulence Intensity; Hot Test.*

1. Introduction

With the rapid improvement in people's living standards, the amount of waste produced in the world is also on an increasing trend. Waste disposal has become a common problem faced by the whole world [1, 2]. The traditional landfill method has been replaced by incineration due to disadvantages such as land occupation and high cost. In terms of urban waste disposal, people have accumulated a lot of experience [3]. However, limited information is available in the literature concerning the incineration of Rural Solid Waste (RSW) [4]. RSW is a fuel with high moisture, high volatility and low calorific value [5, 6], and hence it is not suitable for long-distance transportation and should be disposed in-situ. Therefore, it is required to design a special incinerator for the in-situ disposal of RSW.

In China, there is an urgent need for RSW to be treated in-situ by combustion in rural domestic waste and crop stalks. Due of huge rural area in China, RSW generation rates are rapidly increasing. Therefore, it is necessary to design an incinerator fueled by the rural domestic waste for rural users. RSW is a low calorific value solid fuel similar to inferior coal. Thus, the design of the incinerator has many similarities with the coal-fired boiler. As for coal-fired boiler, the moving grate boilers have been widely used due to their wide adaptability to fuels. This is because the moving grate boiler can reduce dependence on expensive crushing equipment. Since RSW is difficult to be crushed, using moving grate incinerator as the combustion equipment is also suitable for the burning of the RSW. The success of grate combustion equipment design mainly depends on determining reasonable configuration of furnace arches and the air distribution within it. However, the calorific value of RSW is much lower than that of coal, and hence the furnace arch structure and combustion air supply mode of incinerator fueled by rural domestic waste are very different from those of coal-fired boilers. Hence, extensive investigations on the furnace arch structure and combustion air supply mode should be carried out in detailed.

Many efforts have been made to design a coal-fired moving grate furnace suitable for RSW. For example, Li et al. [7] carried out experimental investigations to study the mechanism of unsteady combustion related to volatility in a coal-fired moving grate boiler. It has been reported that the unsteady combustion relies on the configuration of arches and the air distributions. Furthermore, Lin et al. [8] have developed a mathematical model for the design and operation of coal-fired moving grate industrial boilers. It has been shown that there is an optimum excess air ratio for bed combustion for any particular type of coal. For the high ash-content coal or waste, the optimum excess air ratio can be as high as 3.0. Yu et al. [9] have developed a mathematical model, using numerical simulation method, for furnace structure design and operation conditions optimization of grate-fired boiler burning straw. The numerical simulation results show that combustion under the oxygen-enriched atmosphere is better than the combustion under conventional air. Lin et al. [10] have pointed out that the ignition of the waste is more difficult due to the high moisture and low calorific value of the waste. The waste

will ignite rapidly and burn out quickly once the evaporation of water in the fuel completes, while the overall temperature of the furnace of grate waste incinerator is relatively low. All of these characteristics are very different from coal. Therefore, the structure design of the waste incinerators is inevitably different from that of the coal-fueled boiler.

Researchers around the world have been using Computational Fluid Dynamics (CFD) based techniques for flow diagnostics within a range of different flow handling systems [11-18]. Wissing et al. [19] have numerically simulated the process of waste drying, volatile precipitation and carbon conversion. The results demonstrate the new insight into the complex interaction of waste movement, waste conversion and gas phase combustion above the bed of grate incinerator. Kurz et al. [20] have numerically investigated the combustion process of wood chips on a layer burning grate furnace by applying Euler-Euler approach. A detailed multiphase description of the combustion chamber in terms of flow, turbulence and heat transfer are obtained. Results show that the waste layer is firstly exposed to fire from the surface and then gradually goes down and spreads to the grate surface. Wang et al. [21] have numerically studied the municipal solid waste incineration in a bed of waste grate incinerator and gas flow field. They hold that the non-gray radiation needs to be taken into account. Mahmoudi et al. [22] have pointed out that many researchers propose a fixed bed reactor model to describe the combustion on a moving grate due to the complex conditions of waste incineration. The main assumption of these studies is that the temperature and concentration gradients of chemical species are negligible along the direction of grate moving compared to that of the gas flow direction. Their results display that fixed-bed model cannot represent the entire process of biomass combustion on a moving grate. Shrinking of waste caused by grate has a considerable effect on the conversion process on a grate. Yao et al. [23] have simulated both combustion and gasification of municipal solid wastes in a full-scale moving grate furnace. Burning characteristics, including burning rate, gas composition, temperature and burning efficiency as a function of operating parameters are investigated. Their investigations explore a new incineration technology and optimize furnace operating conditions. Thunman et al. [24] have simulated the layer combustion characteristics of waste grate incinerator using four-layer model, i.e. the non-reactive fuel layer, reaction layer, residual carbon layer and grate surface layer. Each layer is calculated by using the equations of energy and mass conservation, while the upper space of the waste layer is simulated by using commercial CFD software. Shin and Choi [25] have used a bed reactor to investigate the combustion of simulated waste particles in a grate incinerator. It states that the flame propagation speed, i.e., the rate of progress of the apparent flame zone, is dependent on the air supply rate, the calorific value of the solid fuel, and the particle size. Peters [26] has indicated that the conversion of solid fuel in a packed or in a moving grate has several steps which include drying, pyrolysis, devolatilization, and gasification. Additionally, the conversion process involves several aspects concerning chemistry, physics, thermodynamics, and fluid dynamics. Moreover, many researchers [27-34] have studied the modeling of thermal conversion and packed bed compaction in biomass combustion. The results of the research show that the rubbish layer on the grate should be simulated by dividing into four layers. Furthermore, a one-dimensional transient model is established under spherical coordinates and a single particle of waste is transiently calculated. Frey et al. [31] have studied the combustion characteristics of one-layer waste incinerator. Their results of research prove that, under the prevailing conditions, the burnout of the flue gas is almost completed before entering the first flue duct due to high temperatures, effective mixing and sufficient residence time of the flue gas inside the combustion chamber.

Assis et al. [35] have simulated the possibility of the injection of agricultural waste, like rice husk, sugar cane bagasse, elephant grass, coffee husk and eucalyptus bark, as an alternative fuel for blast furnace whose structure is very different from that of grate incinerator. The results show that it is possible to reduce specific carbon consumption by using waste generated in agriculture. Raj [36] has carried out a study on physical and chemical characterization of common lignocellulosic agricultural residues available in India, such as rice straw, rice husk, cotton stalk, wheat straw, bagasse, mustard stalk, corn cob and jatropha. The results indicate that corn cob has the highest content of cellulose and hemicellulose, which will be the most potent feedback for production of biofuels. However, how to design a grate incinerator fueled by agricultural residues is not mentioned.

Through the review of the related published literature, it can be found that most researchers focus on the simulation study of the waste grate incinerator and the combustion characteristics of agricultural waste. The experimental studies on the incinerator fueled RSW, especially the arch structure and the combustion air distributions of the grate incinerator, have hardly been reported. As we all know, owing to the complexity of the waste combustion, the difference between the numerical simulation results and the test results could be pretty significant. Thus, the simulation results should only be used as referring. It is necessary to carry out experimental studies on the small-scale grate incinerator fueled RSW. This is the main key issues studied in this paper.

In the present research, in order to determine the reasonable structural parameters of grate furnace arch and air dynamic parameters of a small-scale grate RSW incinerator, the aerodynamic characteristics of the grate RSW incinerator under eight different operating conditions are explored through cold test. Furthermore, the correctness of cold test results is verified by hot test in several different working conditions.

2. Experimental Setup

The experimental diagram of the cold test model of a RSW incinerator with full coverage arches and sub-warehouse air supply is shown in figure 1. The furnace shape looks like “L”, the rear arch is horizontal, and the structure of the front arch and the rear arch are fully covered. The detailed dimensions of the cold test model are introduced as follows.

2.1. Angle of front arch (α)

The front arch angle α affects not only the coverage of the front arch, but also the size of the throat between the two arches. It plays an important role in the waste combustion process. In the present study, the angles of the front arch have been chosen to be 45° and 60° respectively, in accordance with the design experience of the furnace arch structure coal-fired boiler [37-39].

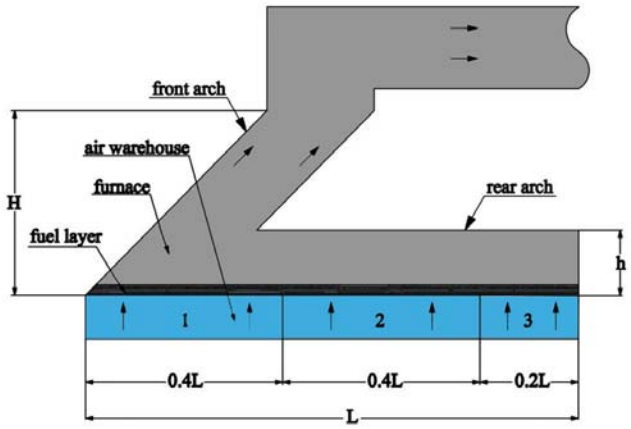

Figure 1. Schematic drawing of the structure of the arches of a waste incinerator

2.2. Height of front arch (H)

H is the height of the front arch, which has an important influence on the effective radiant area of the front arch as well as the flue gas flows between the front arch and the rear arch areas. The height of front arch (H) is designed as two levels of 600mm and 800mm in the experiment.

2.3. Height of rear arch (h)

The height of rear arch (h) refers to the distance between the surface of the waste layer and the rear arch, and this has a direct impact on the combustion aerodynamic properties and the fluid flow resistance in the rear arch region. The arch is horizontally arranged, and the height h is chosen to be as two levels of 240mm and 400mm in the experiment.

2.4. Combustion air supply mode

Appropriate furnace arch structure, combined with corresponding mode of combustion air supply, plays an important role in the design of waste incinerator. According to design experience of coal-fired boiler [39], there are three air warehouses (numbered 1#, 2# and 3#) installed under the grate to provide multi-stage combustion air supply. The proportions of combustion air fed by the three air warehouses are selected as two levels of 40%, 45%, 15% and 30%, 55%, 15% respectively.

2.5. Thickness of the waste layer

It is well recognized that the amount of RSW conveyed into the incinerator varies with the thickness of the waste layer on the grate. Thus, the combustion chamber of the grate incinerator of RSW should be designed with a wide range of load adjustment. Due to high water content and low calorific value of the RSW, the waste layer must be kept at certain thickness in order to maintain the stability of the combustion. It should be stressed here that the thickness of the waste layer cannot be too high in case it should affect the combustion air supply. After comprehensive consideration, the waste layer thickness is determined as two levels of 375mm and 500mm in the present study.

2.6. Fuel properties

In order to study the fuel adaptability, two different types of RSW with different compositions and significant difference in calorific value are tested in the present work. Waste 1 is the rural domestic waste taken from the rural garbage dump; Waste 2, which will be described in detail below, is the mixture of rural domestic waste and crop stalks. The compositions of these two types of waste analyzed by ourselves are shown in table 1.

3. Experimental Procedure

The cold experimental model is made of Plexiglas. Meanwhile, the cold air enters into the model through the air warehouses as the working medium and positive pressure is formed in the test model. At the beginning of the experiment, the cold air passes through the flow regulating valve and enters into combustion air warehouses under the grate, and then comes into the furnace chamber. There are many measuring points located in the side wall of the furnace chamber. Hot wire anemometers, thermocouples and pressure gauges are connected to the measuring points. The precision of the hot wire anemometer is 0.01m/s. The precision of the thermocouples is 0.1K. The thermocouples are connected to Agilent34970A. The devices can record the data every 5 minutes.

The cold test system is shown in figure 2; the specific locations of the numbered measuring points are shown in figure 3. The probes in these small holes on the surface of the Plexiglas are arranged to measure the flow velocity of cold air. The temperature and pressure of the cold air are 20ºC and 1500Pa, respectively.

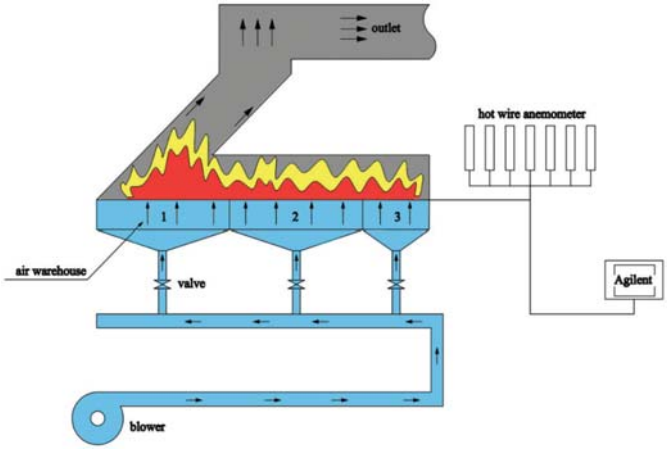

Figure 2. Cold test setup

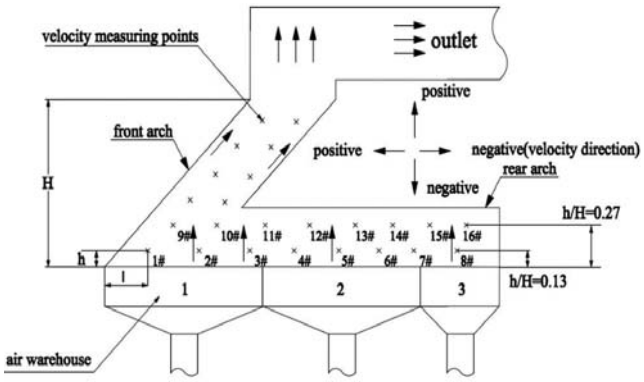

Figure 3. Layout of measuring points

3.1. Cold test of the incinerator

The dimensions of the grate area of the cold test model are: 2.0m × 0.35m = 0.7m^2. According to the references [38-41], the grate and the fuel layer can be simulated by using a perforated plate or a steel wire mesh. Since the combustion is mainly concentrated on the surface of the waste layer, the generated flue gas will rise along the entire grate surface.

Table 1. The compositions of the two types of fuel

Fuel type	C_{ar} (%)	H_{ar} (%)	S_{ar} (%)	O_{ar} (%)	N_{ar} (%)	Cl_{ar} (%)	A_{ar} (%)	W_{ar} (%)	$Q_{net.v.ar}$ (kJ/kg)
Waste 1	11.3	1.75	0.32	8.43	0.37	0.17	28.86	48.89	3340
Waste 2	20.6	3.20	0.60	14.6	0.50	0.34	22.76	37.40	7535

Since the effect of the gas jet of the perforated plate is much stronger than that of the steel wire mesh, the steel wire mesh is selected in the test for simulation in order to reduce the influence of the jet effect.

3.2. Design of cold test conditions

The present work is to design the test conditions based on the principle of the orthogonal experiment. This can not only obtain the calculation results of typical working conditions, but also control the number of test conditions within a reasonable range which can be accepted easily. As a result, a six-factor, two-level orthogonal table (table 2) is obtained by selecting the L8 (27) orthogonal table. The table of cold test conditions can be obtained by changing the levels in table 2 to the specific values, as listed in table 3.

Cold test should be carried out in a self-modeled region. According to the references [37, 39], the equivalent diameter of the rear arch outlet is chosen as the characteristic parameter. For the eight experimental conditions in the present study, the flue gas flow generated at different positions on the grate is simulated by selecting different kinds of waste changing the thickness of the waste layer on the grate and using different air supply mode. The critical Reynolds numbers at the rear arch outlet are calculated and listed in table 4.

It can be clearly observed from table 4 that the critical Reynolds numbers at the rear arch outlet are all greater than the conventional recommended critical Reynolds number (1.5×10^4) in turbulent flow [37, 39], and hence, it can be considered that the cold test condition is within the range of the self-modeled zone ($Re_{outlet} > Re_{cr}$).

Table 2. L8 (27) Orthogonal experiment table

Test Condition	Fuel type	Front arch angle (α)	The height of front arch (H)	The height of rear arch (h)	Air supply mode	Thickness of the waste layer
1	1	1	1	1	1	1
2	1	1	1	2	2	2
3	1	2	2	1	1	2
4	1	2	2	2	2	1
5	2	1	2	1	2	1
6	2	1	2	2	1	2
7	2	2	1	1	2	2
8	2	2	1	2	1	1

Table 3. Cold test conditions

Test Condition	Fuel type	Front arch angle (α)	Height of front arch (H)	Height of rear arch (h)	Air supply mode	Thickness of the waste layer
GK01	Waste1	45°	600mm	240mm	40%,45%,15%	375mm
GK02	Waste1	45°	600mm	400mm	30%,55%,15%	375mm
GK03	Waste1	60°	800mm	240mm	40%,45%,15%	500mm
GK04	Waste1	60°	800mm	400mm	30%,55%,15%	500mm
GK05	Waste2	45°	800mm	240mm	30%,55%,15%	375mm
GK06	Waste2	45°	800mm	400mm	40%,45%,15%	375mm
GK07	Waste2	60°	600mm	240mm	30%,55%,15%	500mm
GK08	Waste2	60°	600mm	400mm	40%,45%,15%	500mm

Table 4. Critical Reynolds numbers (Re_{outlet}) at the rear arch outlet

Test Condition	Fuel type	Warehouse 1	Warehouse 2	Warehouse 3	Fuel thickness	Re_{outlet}
GK01	Waste1	45°	600mm	240mm	40%,45%,15%	375mm
GK02	Waste1	45°	600mm	400mm	30%,55%,15%	375mm
GK03	Waste1	60°	800mm	240mm	40%,45%,15%	500mm
GK04	Waste1	60°	800mm	400mm	30%,55%,15%	500mm
GK05	Waste2	45°	800mm	240mm	30%,55%,15%	375mm
GK06	Waste2	45°	800mm	400mm	40%,45%,15%	375mm
GK07	Waste2	60°	600mm	240mm	30%,55%,15%	500mm
GK08	Waste2	60°	600mm	400mm	40%,45%,15%	500mm

4. Analysis of cold tests

It is known that the front arch controls the radiation ignition. The flame is not the only heat source because the main combustion zone adjacent to the drying zone is of very high temperature, a large area and blackness as well. The main combustion zone constantly releases large amount of heat. Although this part of the heat cannot be radiated directly to the new fuel, it can be passed to the new fuel through the re-radiation of front arch. According to [39-41], the radiation heat transfer of the front arch accounts for more than 70% of the total heat transfer in the front arch which plays a major role in the ignition of the new fuel. Both the front arch length L and height H have significant effects on radioactive heat transfer, but the front arch length L plays a dominant role. This is because when other factors, such as H, α and h, remain constant, the increase of L can substantially increase the wall area of the front arch, further increasing the "transport capacity" of the heat. However, the increase of H can only increase the side wall area of the arch, and the radiation angle coefficient of the side wall is small for the new fuel layer. The absolute value of the direct flame radiation is very small (only about 10% of total heat [41-42]). This is exactly the same as the results of experiments we have carried out. Therefore, dimension of the front arch should be lower and longer. The front arch coverage ratios of test condition 3, 4, 7, 8 are far less than those of test condition 1,2,5,6. As the references [43-44] have pointed out that the radiant heat transfer in arch area is much larger than that in convective heat transfer because the particle size of waste is much larger than 10mm. The correctness of this conclusion is also confirmed by results of experiments we have done. The difference between radiant heat transfer and convective heat transfer is more than five times, while the heat flux density of furnace arch is about twice of that of flue gas. In other words, the front arch should have a larger wall area to ensure radiation heat transfer. Therefore, the furnace arch structures of conditions 3,4,7,8 are not ideal structures since they cannot meet the requirements of radiation heat. The current work mainly carries out the study of cold test with test conditions 1,2,5,6.

4.1. Distribution of airflow velocity

In order to understand the aerodynamic characteristics of the arch area, to judge the performance of the furnace arch, and to determine the reasonable combustion air supply mode, the measurement of velocity field can be used to determine the distribution of airflow in the furnace. The velocity distributions of the two cross sections with relative height of h / H = 0.13 (1 # ~8 # measuring point) and relative height of h / H = 0.27 (9 # ~16# measuring point) along the length of the grate are shown in figures 4 to 7.

Figure 4 depicts the vertical velocity distributions of four different test conditions in the cross section of h/H = 0.13 and it shows that the overall trend of the vertical velocity distribution is from low to high and then low. The maximum value is at the 3 # measuring point. The reason is that the 3# measuring point locates in the space of smooth flow, and the airflow under the front and rear arch converges can exit smoothly. The minimum value appears at 8# measuring point because it locates at the end of the grate where the burning of the waste has ceased. However, the vertical velocities of test conditions 5 and 6 are much higher than those of test conditions 1 and 2, which indicates that flue gas clogging will not occur at the arch region. It is an ideal condition and favorable for the safe operation of the waste incinerator.

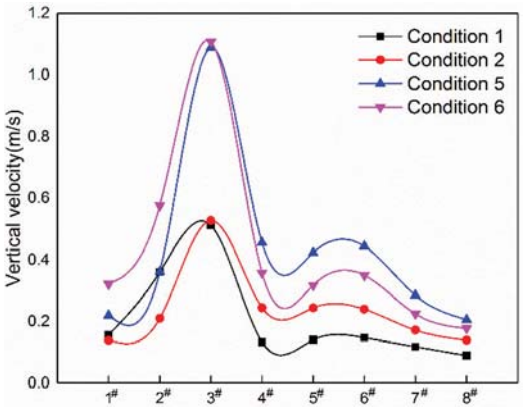

Figure 4. Vertical velocity distribution in the cross section of h / H = 0.13 (1# ~8# measuring point)

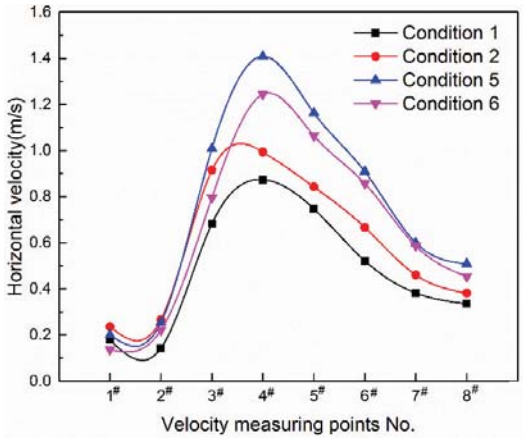

Figure 5. Horizontal velocity distribution in the cross section of h / H = 0.13 (1# ~8# measuring point)

Figure 5 depicts the horizontal velocity distribution in the cross section of h / H = 0.13 and it shows that the overall trend of the vertical velocity distribution is also from low to high and then low. The maximum value appears at 4 # measuring point, and the minimum value is at measuring point 1# (0.2m/s). It indicates that the flue gas under rear arch can enter into the region of front arch at measuring point 1#. Meanwhile, the horizontal velocity doesn't appear any negative value, this means that the flue gas doesn't form a rotating and return flow in the front arch area. The fluid flow in the furnace keeps L-shaped flow. The horizontal velocities of test conditions 5 and 6 are much higher than those of test conditions 1 and 2, which shows that the high-temperature flue gas rushes out of the rear arch at a higher speed and goes deep into the front arch region. Meanwhile, it does not go straight to the front arch and forms excellent flue gas fullness.

The vertical velocity distribution in the cross section of h / H = 0.27 (see figure 6) shows the similar trend to figure-4 and the maximum value at 10 # measuring point is higher than that of at measuring point 3# (see figure-4). The reason is that the measuring point 10# is closer to throat of furnace arch and the flow resistance is lower. Compared with test conditions 5 and 6, the aerodynamic characteristic of test condition 5 is obviously better. The horizontal velocity of each measuring point of test condition 5 is higher than that of condition 6 in h/H=0.13 and h/H=0.27 sections when the air flow are reduced from 40% to 30% in air warehouse 1#, and increased from 45% to 55% in air warehouse 2# in these two test conditions. The turning position of air from outlet of rear arch is advanced towards the front area of furnace, which can effectively raise the level of temperature, enhance the transfer of radiation and convection heat to RSW,

accelerate the evaporation and drying of fuel moisture and maintain stability of ignition and combustion.

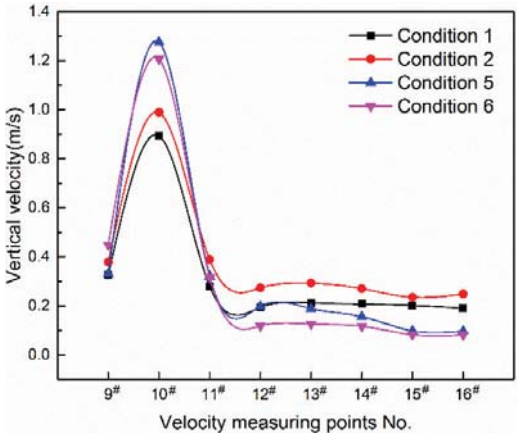

Figure 6. Vertical velocity distribution in the cross section of h / H = 0.27 (9 # ~16# measuring point)

Figure 7 depicts the trend of horizontal velocity distribution in cross section of h/H=0.27 is similar to the section of h/H=0.13(see figure-5). The horizontal velocity reaches the maximum value of 2.5m/s at 11# measuring point, which is much higher than the value at 4# measurement point (1.5m/s) in figure-5. This means the penetration ability of the flue gas from the outlet of rear arch is significantly strengthened in cross section of h /H = 0.27 compared with that of h /H = 0.13 section.

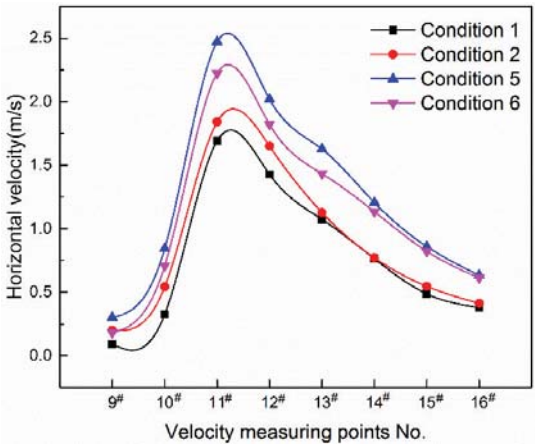

Figure 7. Horizontal velocity distribution in the cross section of h / H = 0.27 (9 # ~16# measuring point)

From the cold test results, it can be perceived that it is difficult for the flue gas to rotate and return. The flue gas moves in L-shaped way. Likewise, it can be observed from the velocity profile with test condition 5 that airflow in the whole furnace arch area is evenly distributed, and the flue gas flows in the ideal L-shape. Such structure will not only be able to help accomplish the preheating and the ignition of new fuel, but also avoid the weaknesses that lead to the temperature dropping in whole furnace because of the low-temperature fuel gas in drying zone entering into the main combustion zone. Therefore, furnace arch structure and combustion air supply mode of the test condition 5 have good aerodynamic characteristics. The optimal angle of front arch and the reasonable height of the arches are as follows: H/L=0.333, h/L=0.12, angle of front arch is 45°; The Combustion air supply ratio in front and rear arch is 3:7; combustion air supply ratio in air warehouses (1#, 2# and 3#) is 30%, 55%, and 15%.

4.2. Turbulence distribution

The flue gas turbulence, which has an important influence on the mixing of airflow in arch region and the combustion stability, can accurately reflect aerodynamic conditions in the furnace. The flue turbulence is defined as follows:

$$\varepsilon = \frac{\sqrt{\overline{u'^2}}}{\overline{V}} \times 100\ \% \qquad (1)$$

where $\sqrt{\overline{u'^2}}$ is the root mean square value of pulsating velocity at each measuring point, $\overline{V}$ is the average velocity of each measuring point. The flue gas turbulence is tested by using Testo 425 hot air anemometer with an accuracy of 0.01m/s. The equipment has a monitor that can be read directly through a one-dimension hotline probe and a spherical probe. Figure 8 depicts the distribution of turbulence along the grate in the cross section of h/H=0.13. It shows that the overall distribution of turbulence is from low to high and then low. However, the increase and decrease of turbulence vary greatly and it can be said that the gradient of turbulence is very large. The maximum value occurs in the middle region of rear arch (at 5# measuring point) (see figure 8). The reason could be that the cross section of h/H=0.13 is close to the outlet of air warehouse, and that the airflow from air warehouse 3# and from part of warehouse 2# turns up rapidly at the 5# measuring point, which results in an increase of turbulence.

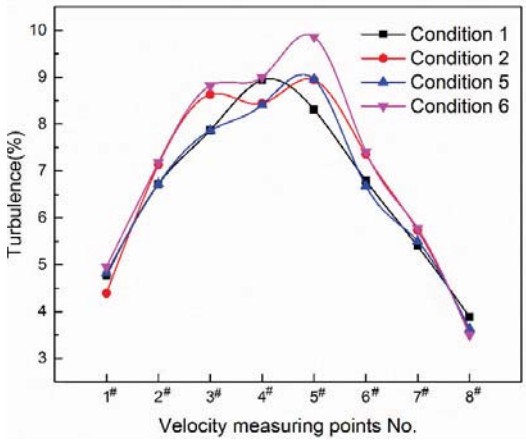

Figure 8. Turbulence distribution in the cross section of h / H = 0.13 (1# ~8# measuring point)

Figure 9 depicts the distribution of turbulence along the grate in the cross section of h / H = 0.27. The turbulence sharply rises from 9 # measuring point to 10 # measuring point. Then, the turbulence descends quickly from 10 # measuring point to 11 # measuring point and a stage of gentle change of distribution of turbulence follows. Again the turbulence descends quickly from 13 # measuring point to 14 # measuring point and a stage of gentle change of distribution of turbulence appears from 15 # measuring point to 16 # measuring point. Because the air flow in the three ware houses is completely mixed at the measuring point of 10# and then turns to the outflow, the turbulence reaches the maximum value at 10# measuring point. This results in larger flow disturbances and the peak of the turbulence appears at this location.

To sum up, the maximum turbulence value along the length of the chain grate appears in the region of l/L= 0.2~0.6. Meanwhile, the region with maximum turbulence value in the furnace is close to the outlet throat of the rear arch. It shows that the area of highest turbulence happens to be where waste fuel burned strongly, which is beneficial to stable combustion of waste, as

well as the precipitation, ignition and burning of volatile in the incinerator bed.

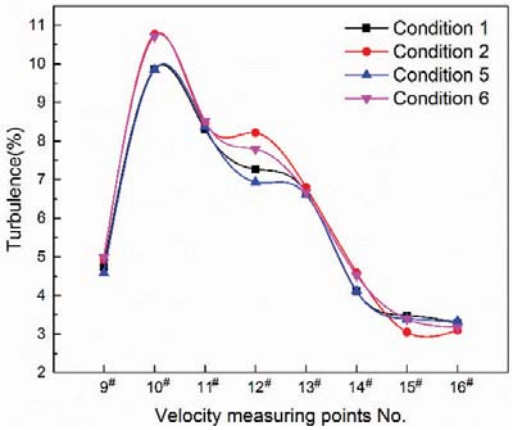

Figure 9. Turbulence distribution in the cross section of h / H = 0.27 (9 # ~16# measuring point)

5. Hot test of the incinerator

The hot test is carried out in a 0.5 t/h small-scale layer burning chain grate furnace. The size of the travelling grate chain is 2 meters in length and 0.35 meter in width. The model of the hot state test is shown in figure 10. Combustion tests are conducted at eight different test conditions corresponding to the cold test, as listed in table2. In order to verify the rationality and applicability of the furnace arch structure proposed in the current work, the temperature distributions in the furnace are measured by using thermocouples whose precision is 0.1K. Figure 11 depicts the arrangement of the temperature measuring points. There are two types of fuel used in the hot test with different components. Waste 1 is taken from the rural waste dump. The analytical results of the composition made by ourselves are shown in table 5. Waste 2 is a mixture of waste 1 and crop stalks. The aim is to increase the calorific value of the RSW to make the combustion of RSW easier. The analysis of crop stalks made by ourselves is shown in Table 6; the mixing ratio and calorific value of mixture fuel are listed in table 7.

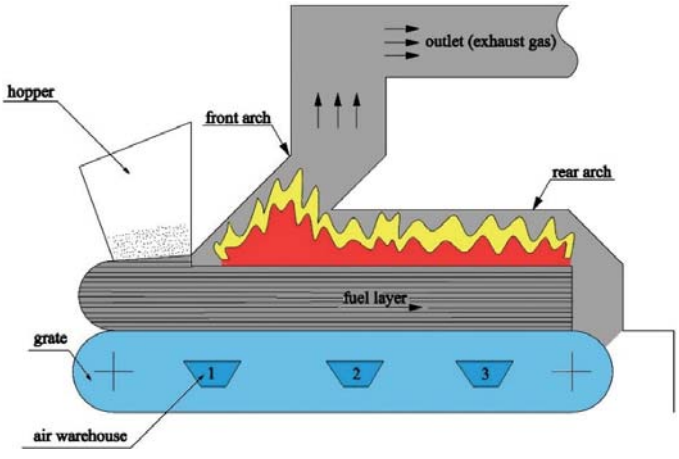

Figure 10. Hot test set up

Figure 12 depicts the temperature profile in the cross section of h / H = 0.13 at eight different test conditions. It shows that the overall trend of the temperature distribution is from low to high and then low. The maximum temperature occurs at measuring point #3 since the location lies in the strong burning region inside the furnace. Meanwhile, the minimum value of temperature appears at measuring point #1 because the location lies in the connection between drying and burning region inside the furnace. On the whole, the change of temperature is generally gentle. However, the temperatures of test conditions 3, 4, 7 and 8 are much higher than those of test conditions 1, 2, 5 and 6, which indicates that high calorific value waste and thicker waste layer are beneficial to combustion of RSW. Test conditions 3, 4, 7 and 8 are ideal conditions, while the thickness of waste layer is more important to the safe operation of the waste incinerator.

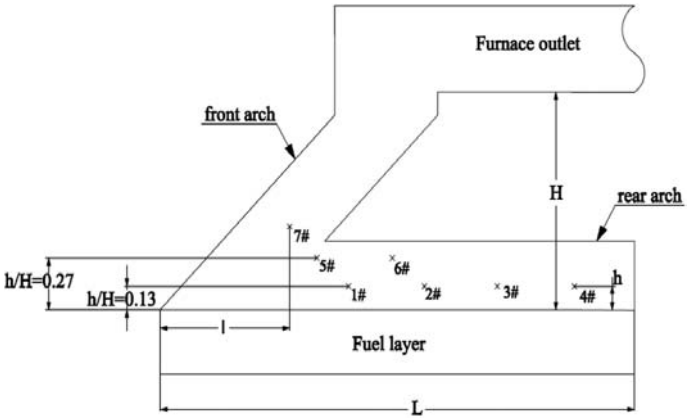

Figure 11. Layout of temperature test points

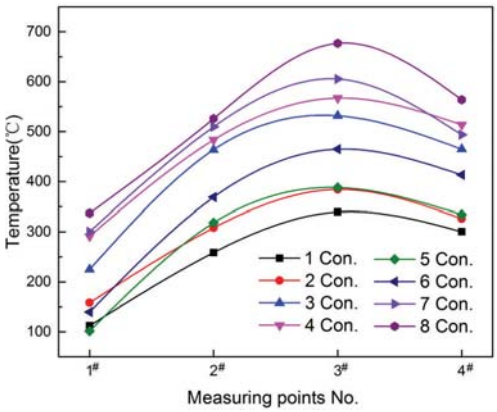

Figure 12. Temperature distribution in the cross section of h / H = 0.13 (1# ~ 4# measuring point)

Figure 13 depicts the temperature of three measuring points in the cross section of h/H=0.27. The maximum temperature appears at measuring point #6 and the minimum value at point # 5. The reason is that the measuring point #6 is located near the outlet under the rear arch, which is the strong burning region. Meanwhile, the location of #5 is under the front arch. The gas flow at this point has dried the waste firstly, and then mixed with the hot flue gas from strong burning region. Therefore, the temperature decreases sharply at measuring point # 5. Because the waste is burned out at the measuring point # 7, the temperature increases at the measuring point # 7. Similarly, the temperatures of test conditions 3, 4, 7 and 8 are much higher than those of test conditions 1, 2, 5 and 6. This confirms the conclusion that the waste layer of the incinerator should be as thick as possible under the condition of not affecting the combustion air supply.

As can be seen from the figure 12 and figure 13, the temperature difference under the rear arch is small, which implies that the combustion in the furnace is stable. These results show that the furnace arch structure can form ideal L-shaped flame and the structure of the arches proposed in present study is suitable for the combustion of the RSW. The hot test result confirms the rationality for the design of the furnace arch of RSW incinerator.

Table 5. Components of waste 1

C_{ar} (%)	H_{ar} (%)	S_{ar} (%)	O_{ar} (%)	N_{ar} (%)	Cl_{ar} (%)	A_{ar} (%)	W_{ar} (%)	$Q_{net.v.ar}$ (kJ/kg)
12.35	1.95	0.34	9.45	0.42	0.2	26.09	49.2	4120

Table 6. Components of the crop stalks

C_{ar} (%)	H_{ar} (%)	S_{ar} (%)	O_{ar} (%)	N_{ar} (%)	Cl_{ar} (%)	A_{ar} (%)	W_{ar} (%)	$Q_{net.v.ar}$ (kJ/kg)
40.12	5.19	0.33	32.76	0.22	0.1	0.3	20.98	1335

Table 7. Components of waste 2

Item	Quality Ratio (%)	Calorific value (kJ/kg)
Waste 1	70	4120
Crop Stalks	30	13351
Waste 2 (mixture)	-	6889

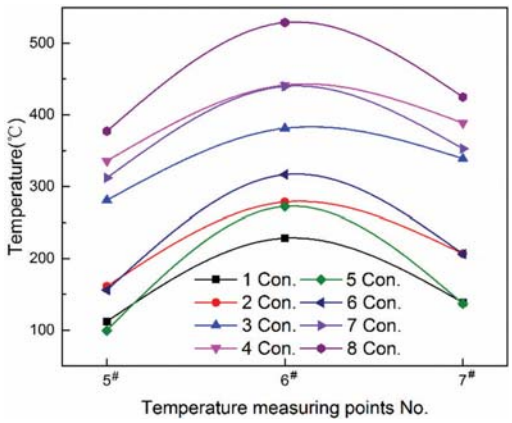

Figure 13. Temperature distribution in the cross section of h/H = 0.27 section (measuring points #5 ~ #7)

6. Conclusions

This study presents a new design of RSW incinerator of L-shaped flame and both cold and hot tests are carried out. The distributions of velocity, turbulence and temperature are obtained. By comparison of different cold test results, the structure of furnace arches with excellent turbulent mixing performance and the reasonable air supply mode are obtained. Through the hot test, it is proved that the furnace arch structure of the RSW incinerator proposed in this paper is reasonable and applicable. Several main findings can be summarized as follows:

1. The results of cold test show that furnace arches structure of L-shaped flame with full coverage front/rear arch and horizontal rear arch can help to achieve good aerodynamic performance in the furnace.
2. Dimensionless structural parameters of the furnace arches are: H/L = 0.333 and h/L = 0 .12 with the front arch angle of 45º.
3. Recommended air supply ratio between the front arch and the rear arch is 3:7. The air supply ratios of 1# 2# 3# air warehouse are 30%, 55%, 15%, respectively.
4. Value of turbulence distribution is small in front and rear region of furnace, while it is large in the region of l/L = 0.25 ~ 0.6 and the maximum value can rise up to 10%.
5. Hot test results show that the cold flue gas in the drying section will not affect the combustion condition in the main combustion zone with the L-shaped flame combustion technology. The arches structure of L-shaped flame can ensure the RSW to be ignited easily and burned stably.

Acknowledgements

This work is supported by the Scientific and Technological Plan of Guangdong Province (Nos. 2010B080701003) and financial support from the University of Hertfordshire, United Kingdom.

References

1. Yang, B.Y. Vida, N.S. and Jim, S. (2007). Converting moving-grate incineration from combustion to gasification-Numerical simulation of the burning characteristics. Waste Management. Volume: 27. 645 – 655.
2. Wang, Y.N. (2010). Study of the status quo of the power generation through the incineration of daily-life refuse in big cities in China and its development. Macroeconomic Research. Volume: 11. 12 – 23.
3. Chen, D. and Tang, M.H. (2010). Practice of power generation through the refuse incineration in Europe and America and its popularization in China. Journal of Chongqing Institute of Science and Technology. Volume: 11. 63 – 64.
4. Kuang, M. Li, Z.Q. Zhu, Q.Y. and Liu, C.L. (2013). Arch- and wall-air distribution optimization for a down-fired 350 MWe utility boiler: A cold-modeling experimental study accompanied by real-furnace measurements. Applied Thermal Engineering. Volume: 54. 226 – 236.
5. Liu, G.K. Chen, Z.C. Li, Z.Q. Li, G.P. and Zong, Q.D. (2015). Numerical simulations of flow, combustion characteristics, and NOx emission for down-fired boiler with different arch-supplied over-fire air ratios. Applied Thermal Engineering. Volume: 75. 1034 – 1045.
6. Zhang, D.L. Meng, C.W. Zhang, H. Zhang, H. Liu, P.Y. Li, Z.H. Wu, Y.X. Lu, J.F. Zhou, W. Ran, S.M. and Zhang, D.H. (2016). Studies on heat flux distribution on the membrane walls in a 600 MW supercritical arch-fired boiler. Applied Thermal Engineering. Volume: 103. 264 – 273.
7. Li, J.J. Luo, Y.H. and Hu, L.Y. (2008). Study on the mechanism of unsteady combustion related to volatile in a coal-fired traveling grate boiler. Applied Thermal Engineering. Volume: 28. 145 – 156.
8. Lin, P.Y. Ji, J.J. Luo, Y.H. and Wang, Y. (2009). A non-isothermal integrated model of coal-fired traveling grate boilers. Applied Thermal Engineering. Volume: 29. 3224 – 3234.
9. Yu, Z.S. Ma, X.Q. and Liao, Y.F. (2010). Mathematical model of combustion in a grate-fired boiler burning straw and effect of operating conditions under air- and oxygen-enriched atmospheres. Renewable Energy. Volume: 35. 895 – 903.

10. Lin, H. and Ma, X.Q. (2012). Simulation of co-incineration of sewage sludge with municipal solid waste in a grate furnace incinerator. Waste Management. Volume: 32. 561 – 567.
11. Asim, T. Oliveira, A. Charlton, M. and Mishra, R. (2019). Improved Design of a Multi-Stage Continuous-Resistance Trim for minimum Energy Loss in Control Valves. Energy. Volume: 174. 954 – 971.
12. Asim, T. Oliveira, A. Charlton, M. and Mishra, R. (2019). Effects of the Geometrical Features of Flow Paths on the Flow Capacity of a Control Valve Trim. Petroleum science and Engineering. Volume: 172. 124 – 138.
13. Asim, T. Algadhi, A. and Mishra, R. (2018). Effect of Capsule Shape on Hydrodynamic Characteristics and Optimal Design of Hydraulic Capsule Pipelines. Journal of Petroleum Science and Engineering. Volume: 161. 390 – 408.
14. Asim, T. Charlton, M. and Mishra, R. (2017). CFD based Investigations for the Design of Severe Service Control Valves used in Energy Systems. Energy Conversion and Management. Volume: 153. 288 – 303.
15. Asim, T. and Mishra, R. (2017). Large Eddy Simulation based Analysis of Complex Flow Structures within the Volute of a Vaneless Centrifugal Pump. Sadhana. Volume: 42. 505 – 516.
16. Asim, T. and Mishra, R. (2016). Optimal design of hydraulic capsule pipelines transporting spherical capsules. Canadian Journal of Chemical Engineering. Volume: 94. 966 – 979.
17. Asim, T. and Mishra, R. (2016). Computational Fluid Dynamics based Optimal Design of Hydraulic Capsule Pipelines Transporting Cylindrical Capsules. International Journal of Powder Technology. Volume: 295. 180 – 201.
18. Asim, T. Mishra, R. Abushaala, S. and Jain, A. (2016). Development of a Design Methodology for Hydraulic Pipelines Carrying Rectangular Capsules. International Journal of Pressure Vessels and Piping. Volume: 146. 111 – 128.
19. Wissing, F. Wirtz, S. and Scherer, V. (2017). Simulating municipal solid waste incineration with a DEM/CFD method– Influences of waste properties, grate and furnace design. Fuel. Volume: 206. 638 – 656.
20. Kurz, D. Schnell, U. and Scheffknecht, G. (2013). Euler-Euler simulation of wood chip combustion on a grate–effect of fuel moisture content and full scale application. Progress in Computational Fluid Dynamics. Volume: 13. 322 – 332.
21. Wang, J.F. Xue, Y.Q. Zhang, X.X. and Shu, X.R. (2016). Numerical study of radiation effect on the municipal solid waste combustion characteristics inside an incinerator. Waste Management. Volume: 44. 116 – 124.
22. Mahmoudi, A.H. Besseron, X. Hoffmann, F. Markovic, M. and Peters, B. (2016). Modeling of the biomass combustion on a forward acting grate using XDEM. Chemical Engineering Science. Volume: 142. 32 – 41.
23. Yao, B.Y. Sharifi, V.N. and Swithenbank, J. (2007). Converting moving-grate incineration from combustion to gasification-Numerical simulation of the burning characteristics. Waste Management. Volume: 27. 645 – 655.
24. Thunman, H. (2013). Modelling and verifying experiments on the whole furnace, in principles and models of solid fuel combustion. PhD Thesis, Chalmers University of Technology, Sweden.
25. Shin, D. and Choi, S. (2000). The combustion of simulated waste particles in a bed. Combustion and Flame. Volume: 121. 167 – 180.
26. Peters, B. (2003). Thermal Conversion of Solid Fuels. Mechanical Engineering. Volume: 8. 67.
27. Gómez, M.A. Porteiro, J. Patiño, D. and Míguez, J.L. (2014). CFD modelling of thermal conversion and packed bed compaction in biomass combustion. Fuel. Volume: 117. 716 – 732.
28. Adams, T.N. (1980). A simple fuel bed model for predicting particulate emissions from a wood waste boiler. Combustion and Flame. Volume: 39. 225 – 239.
29. Beckmann, M., Scholz, R., (1995), Simplified mathematical model of combustion in stoker systems in Proc. 3rd European Conference on Industrial Furnaces and Boilers, Porto, Potrugal.
30. Karim, M., Naser, J., (2014), Progress in Numerical Modeling of Packed Bed Biomass Combustion in Proc. 19th Australasian Fluid Mechanics Conference (AFMC), Melbourne, Australia.
31. Frey, H.H. Peters, B. Hunsinger, H. and Vehlow, J. (2003). Characterization of municipal solid waste combustion in a grate furnace. Waste Management. Volume: 23. 689 – 701.
32. Lin, H. and Ma, X.Q. (2012). Simulation of co-incineration of sewage sludge with municipal solid waste in a grate furnace incinerator. Waste Management. Volume: 32. 561 – 567.
33. Sakai, S. and Hiraoka, M. (2000). Municipal solid waste incinerator residue recycling by thermal processes. Waste Management. Volume: 20. 249 – 258.
34. Jiang, S., Lv, W., Gao, W.X., Qi, G.L., Zhang, S.S., Li, Y.Q., (2017), Study on the Influence of Furnace Arch Structure on the Combustion Characteristics of Chain Furnace in Proc. 2nd International Conference on Electrical, Automation and Mechanical Engineering, Shanghai, China.
35. Assis, C.F.C. Tenorio, J.A.S. Assis, P.S. and Nath, N.K. (2014). Experimental Simulation and Analysis of Agricultural Waste Injection as an Alternative Fuel for Blast Furnace. Energy Fuels. Volume: 28. 7268 – 7273.
36. Raj, T. Kapoor, M. Gaur, R. Christopher, J. Lamba, B. and Tuli, D.K. (2015). Physical and Chemical Characterization of Various Indian Agriculture Residues for Biofuels Production. Energy Fuels. Volume: 29. 3111 – 3118.
37. Chu, J.F. (2014). Numerical simulation study on influence of arch and air distribution mode for combustion performance in reciprocating furnace. PhD Thesis, Harbin Institute of Technology, Harbin, China.
38. Qian, H.Q. and Miao, Z.Q. (2007). Numerical of air flow in arches of grate stokers. Energy conservation. Volume: 26. 20 – 21.
39. Huang, X.X. (1984). Characteristics of furnace arch of fire furnace. Chinese Journal of Power Engineering. Volume: 2. 22 – 28.
40. Ma, X.Q. Yang, Z.L. and Chen, L.Q. (1996). The methods of raising the efficiency of waste incineration power generation. New Energy. Volume: 18. 42 – 45.
41. Miu, Z.Q. Huang, X.X. Yang, D. Yu, G.Q. and Huang, J.W. (1996). Study on Heat Transfer and Its Effect on the Fire Bed Burning in Arch Rear Area of Fire-bed Furnace. Industrial Boiler. Volume: 4. 18 – 24.
42. Hui, S.E. Xu, T.M. Liu, Z.J. and Jiang, H.Z. (1994). A New Method for Designing a Fire Hearth Furnace Arch with Strongly Actuated α Flames. Thermal Power Engineering. Volume: 5. 280 – 284.
43. Ma, X.Q. (1997). Design method for waste incineration boiler and its combustion stability. New Energy. Volume: 19. 9 – 12.
44. Cen, K.F. and Fan, J.R. (1991). Combustion Fluid Dynamics, 1st ed., China Water Power Press, Beijing, China.